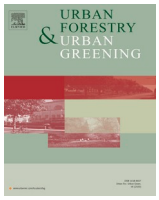
Urban Forestry & Urban Greening 112 (2025) 128970



Contents lists available at ScienceDirect

Urban Forestry & Urban Greening

journal homepage: www.elsevier.com/locate/ufug



# Climate drivers of dieback in Mediterranean urban pine forests

Antonio M. Cachinero-Vivar [a,b], Oscar Pérez-Priego [a,b], J. Julio Camarero [c,*]

[a] Forestry Engineering Department, School of Agriculture and Forestry, University of Córdoba, Laboratory of Dasometry and Forest Management, Edif. Leonardo da Vinci, Campus de Rabanales s/n, Córdoba 14071, Spain
[b] Instituto Interuniversitario del Sistema Tierra en Andalucía, Centro Andaluz de Medio Ambiente (IISTA-CEAMA), Avenida Mediterráneo, S/N, Granada 18006, Spain
[c] Instituto Pirenaico de Ecología (IPE-CSIC), Avda. Montañana 1005, Zaragoza 50192, Spain

ARTICLE INFO

*Keywords:*
Dendroecology
Drought stress
Forest die-off
Málaga
*Pinus halepensis*

ABSTRACT

Droughts trigger forest dieback worldwide, but these events are still understudied in cities. However, conditions of urban forests can aggravate drought stress due to heat island effects, poor growing conditions or lack of management. We investigated a recent dieback event affecting four *Pinus halepensis* Mediterranean forests located in Málaga, south eastern Spain. We sampled declining (D) and non-declining (ND) trees showing high and low defoliation levels, respectively, and measured their diameter, stem water content (SWC) and radial growth. We used dendrochronology to obtain basal area increment (BAI) series in 40 trees per forest corresponding to D and ND trees growing in N- and S-oriented slopes. These data were correlated with climate variables, teleconnection indices such as the North Atlantic Oscillation (NAO) index and a drought index. Remote sensing indices were used to evaluate changes in cover and greenness. We found that D trees significantly grew more than ND trees in three out of four forests, regardless slope orientation. However, D trees showed a stronger growth decline in the past 10 years and lower SWC than ND trees. Growth was enhanced by high precipitation in the prior December and high minimum temperatures in April. Long winter droughts constrained growth. The dieback was triggered by very warm and dry conditions starting in the winter 2021–2022 and leading to sharp declines in cover and growth from 2022 to 2024. Such dry winter conditions were linked to positive NAO phases. Fast-growing trees with lower SWC were prone to show dieback in response to severe and long winter droughts. These two characteristics could be further explored as early-warning signals of dieback and tree death. Adaptive urban silviculture should consider thinning but also planting tree and shrub species showing higher drought tolerance.

## 1. Introduction

By 2050, about 67 % of the population worldwide will live in urban areas and will consume more than 70 % of global energy (UNDESA, 2014). As global temperatures continue rising and urban population increases, heat islands will strengthen causing harmful health and environmental effects (Hibbard et al., 2017; Huang et al., 2019). Such extra warming rate due to urban expansion may be partially offset by landscape greening through the enhanced evaporation capability of trees (Bowler et al., 2010; Li et al., 2019; Liu et al., 2022). However, the cooling effect of urban greening depends on background climate conditions and vegetation type, spatial arrangement and tree structural attributes, among other factors (Leuzinger et al., 2010; Rakoto et al., 2021). Therefore, urban greening may show a limited capacity to mitigate local warming in cities with urban forests dominated by species vulnerable to climate extremes such as droughts (Esperon-Rodriguez et al., 2022).

The cooling effect of urban forests may be compromised by drought-

*Abbreviations:* AC1, First-Order Autocorrelation of tree-ring width; ANOVA, Analysis of Variance; BA, Basal area $m^2$ $ha^{-1}$; BAI, Basal area increment $cm^2$ $yr^{-1}$; $BAI_{10}$, Basal area increment in the last 10 years $cm^2$ $yr^{-1}$; $BAI_{20}$, Basal area increment in the last 20 years $cm^2$ $yr^{-1}$; D, Declining Trees; DBH, Diameter at breast height cm; EPS, Expressed Population Signal; H, Tree height m; MS, Mean sensitivity relative change in width between consecutive rings; NAO, North Atlantic Oscillation index; ND, Non-Declining Trees; NDVI, Normalized Difference Vegetation Index; KNDVI, kernel NDVI; Pr, Total precipitation mm; $R_{bar}$, Mean correlation between trees; RWI, Ring-width index; SPEI, Standardized Precipitation and Evapotranspiration Index; SWC, Stem Water Content %; Tn, Mean minimum temperature °C; TukeyHSD, Tukey's Honestly Significant Difference test; Tx, Mean maximum temperature °C; TRW, Tree-ring width mm; VPD, Vapor Pressure Deficit kPa; WeMO, Western Mediterranean Oscillation index.

* Corresponding author.
*E-mail addresses:* o02cavia@uco.es (A.M. Cachinero-Vivar), g72pepro@uco.es (O. Pérez-Priego), jjcamarero@ipe.csic.es (J.J. Camarero).

https://doi.org/10.1016/j.ufug.2025.128970
Received 11 March 2025; Received in revised form 10 July 2025; Accepted 18 July 2025
Available online 19 July 2025
1618-8667/© 2025 The Authors. Published by Elsevier GmbH. This is an open access article under the CC BY license (http://creativecommons.org/licenses/by/4.0/).

**Table 1**
General characteristics of the Aleppo pine forests sampled in Málaga, south eastern Spain. Values are means (standard deviation) calculated for non-declining (ND) and declining (D) trees. Abbreviations: DBH, diameter at breast height; and SWC, stem water content. Different letters indicate significant differences between vigor classes within each site (Tukey HSD tests, $p < 0.05$).

| Site | Area (ha) | Stem density (No. ha-1) | Orientation | Vigor class | Plot code | Latitude (ºN) | Longitude (ºW) | DBH (cm) | SWC (%) | Height (m) |
|---|---|---|---|---|---|---|---|---|---|---|
| Gibralfaro | 37.78 | 212 | North | ND | GNND | 36.7238 | 4.4094 | 24.38 (1.91) | 33.28 (3.31)b | 12.2 (3.2) |
| | | | | D | GND | 36.7238 | 4.4082 | 24.26 (1.85) | 27.09 (2.77)a | 11.8 (2.8) |
| | | | South | ND | GSND | 36.7225 | 4.4113 | 22.26 (4.01) | 28.33 (1.44)b | 12.1 (2.9) |
| | | | | D | GSD | 36.7224 | 4.4095 | 21.92 (2.94) | 24.11 (1.17)a | 11.7 (1.8) |
| Morlaco | 17.95 | 183 | North | ND | MNND | 32.7242 | 4.3862 | 23.18 (1.77) | 29.37 (2.54) | 12.1 (3.0) |
| | | | | D | MND | 32.7247 | 4.3852 | 23.72 (1.42) | 25.76 (1.28) | 11.9 (1.8) |
| | | | South | ND | MSND | 36.7240 | 4.3836 | 22.54 (1.46) | 28.14 (2.94) | 12.0 (2.8) |
| | | | | D | MSD | 36.7236 | 4.3850 | 23.16 (1.44) | 24.40 (2.09) | 11.7 (1.6) |
| San Antón | 359.95 | 32 | North | ND | SNND | 36.7446 | 4.3576 | 27.28 (1.06) | 31.08 (1.05) | 9.2 (2.2) |
| | | | | D | SND | 36.7453 | 4.3582 | 27.62 (1.06) | 29.41 (6.34) | 8.8 (1.5) |
| | | | South | ND | SSND | 32.7414 | 4.3627 | 26.96 (1.02) | 28.57 (0.89) | 9.0 (2.0) |
| | | | | D | SSD | 36.7411 | 4.3570 | 27.52 (0.68) | 26.85 (6.55) | 8.6 (1.4) |
| Victoria | 48.63 | 66 | North | ND | VNND | 36.7329 | 4.4099 | 26.66 (3.70) | 31.23 (1.17)b | 13.6 (3.0) |
| | | | | D | VND | 36.7336 | 4.4080 | 26.92 (3.71) | 26.43 (0.62)a | 12.8 (2.9) |
| | | | South | ND | VSND | 36.7310 | 4.4109 | 24.86 (2.74) | 26.11 (1.04)b | 13.0 (2.9) |
| | | | | D | VSD | 36.7313 | 4.4093 | 25.04 (2.58) | 23.73 (0.69)a | 12.7 (2.8) |

induced stress leading to growth decline, widespread canopy dieback and tree mortality as it has been observed in cities around the world (Chen et al., 2011; Gillner et al., 2013; Bialecki et al., 2018; Rötzer et al., 2021; Marchin et al., 2022). Hotter droughts and heat waves are triggering forest dieback and tree mortality events worldwide (Hammond et al., 2022). Urban trees may also be affected by hot-dry events which may be aggravated by 'heat islands' and 'dry islands' effects in cities (Czaja et al., 2020; Esperon-Rodriguez et al., 2022). Note that both hot and low-humidity air increases the vapor pressure deficit (VPD), a primary factor constraining tree transpiration (Grossiord et al., 2020). Consequently, urban forests can have higher water demand than comparable natural forests (Pataki et al., 2011). Thus, the rising intensity, duration, and frequency of heatwaves and droughts observed in some seasonally dry regions such as the Mediterranean Basin (Cramer et al., 2018), will make it essential to drought-tolerant tree and shrub species in progressively more stressed urban forests. Such selection of resilient species must consider the limiting growing conditions of many urban forests and their complex management, which depends on multiple factors - including air pollution, soil depth and permeability, water accessibility, species functional traits - in addition to the microclimate. These interconnected factors collectively shape the viability of urban forests (Vogt, 2020). In this sense, retrospective proxies of long-term tree functioning such as tree rings have provided evidence-based data to improve management decisions in urban forestry (Farrell et al., 2015; Miyahara et al., 2022).

Recent drying in urban areas have been shown to constrain tree radial growth (Helama et al., 2012; Gillner et al., 2013; David et al., 2015; Dervishi et al., 2022; Moser et al., 2016; Franceschi et al., 2023; Wu et al., 2025). However, a comparison of urban and rural trees found that tree growth in cities was enhanced due to heat-island effects (Pretzsch et al., 2017). These discrepancies may be reconciled by considering species' and sites' characteristics (e.g., orientation) related to drought tolerance (Gregg et al., 2003; Roy et al., 2012; Gillner et al., 2014; Camarero et al., 2015a). Site orientation strongly influences solar radiation exposure, soil moisture dynamics and evaporative demand. In Mediterranean-climate pine forests, south-facing slopes receive more insolation and dry out earlier in summer, leading to higher water stress and increased mortality during drought (Camarero et al., 2015a, 2015b). By explicitly including orientation in the analyses, we can capture those microclimatic gradients that modulate tree growth responses to climate stress and better forecast dieback patterns.

Here, we aim to use tree-ring data as a biomonitoring tool to infer the main climatic drivers of a recent forest die-off episode affecting urban parks in the Málaga city located in the Mediterranean coast of southeastern Spain. There, the affected parks were dominated by Aleppo pine (*Pinus halepensis* Mill.) plantations, which were carried out in drought-prone Spanish urban and rural areas during the mid-20th century (Maestre and Cortina, 2004). These plantations have been shown to be susceptible to drought stress in semi-arid areas, where die-off and high mortality rates were observed and linked to widespread xylem cavitation (García de la Serrana et al., 2015; Morcillo et al., 2022). The impact of hotter droughts on such planted pine forests can be further exacerbated by inadequate management leading to dense and homogeneous stands (Navarro-Cerrillo et al., 2023). Our specific aims are: (i) to reconstruct the growth patterns of affected urban pine forests, and (ii) to determine the main site conditions through a terrain analysis, paying particular attention to orientation, and climate drivers of die-off episodes starting in 2022. We followed a multi-proxy approach by combining tree-ring data with remote sensing indices describing the dynamics of tree cover and greenness (Tucker, 1979). By identifying key climatic risk factors, microclimatic factors related to orientation and the increased vulnerability of fast-growing individuals, these findings furnish actionable recommendations, which include targeted monitoring and site-specific management interventions, to bolster the resilience of urban pine forests against severe droughts and progressive aridification.

## 2. Materials and methods

### 2.1. Study sites

The study sites are four urban forests dominated by Aleppo pine and located in the Málaga city, Andalusia, south eastern Spain. In this city, urban forests and parks occupy ca. 611 ha. The urban and forests and parks account for over 70 % of the city green infrastructure. We selected four urban forests (Gibralfaro, Morlaco, San Antón, and Victoria) for sampling because they showed different size and were located at different distances from the city center (Table 1). In addition to Aleppo pine, other tree species were planted in the forest edges or in dry streams including *Eucalyptus globulus*, *Eucalyptus camaldulensis* and *Cupressus sempervirens*. Other planted or naturally established trees include *Ceratonia siliqua*, *Olea europaea*, *Prunus dulcis*, *Celtis australis*, *Quercus ilex*, *Punica granatum*, and *Crataegus monogyna*. The understory is dominated by several shrub species such as *Juniperus phoenicea*, *Juniperus oxycedrus*, *Nerium oleander*, *Ulex parviflorus*, *Rhamnus alaternus*, *Pistacia lentiscus*, *Salvia rosmarinus*, *Cistus monspeliensis*, *Genista umbellata*, *Myrtus communis*, *Lavandula* spp., and *Retama* spp. Dwarf fan palms (*Chamaerops humilis*) are also abundant.

In Málaga, maximum and minimum temperatures have increased significantly ($p < 0.001$) across all seasons, while summer precipitation

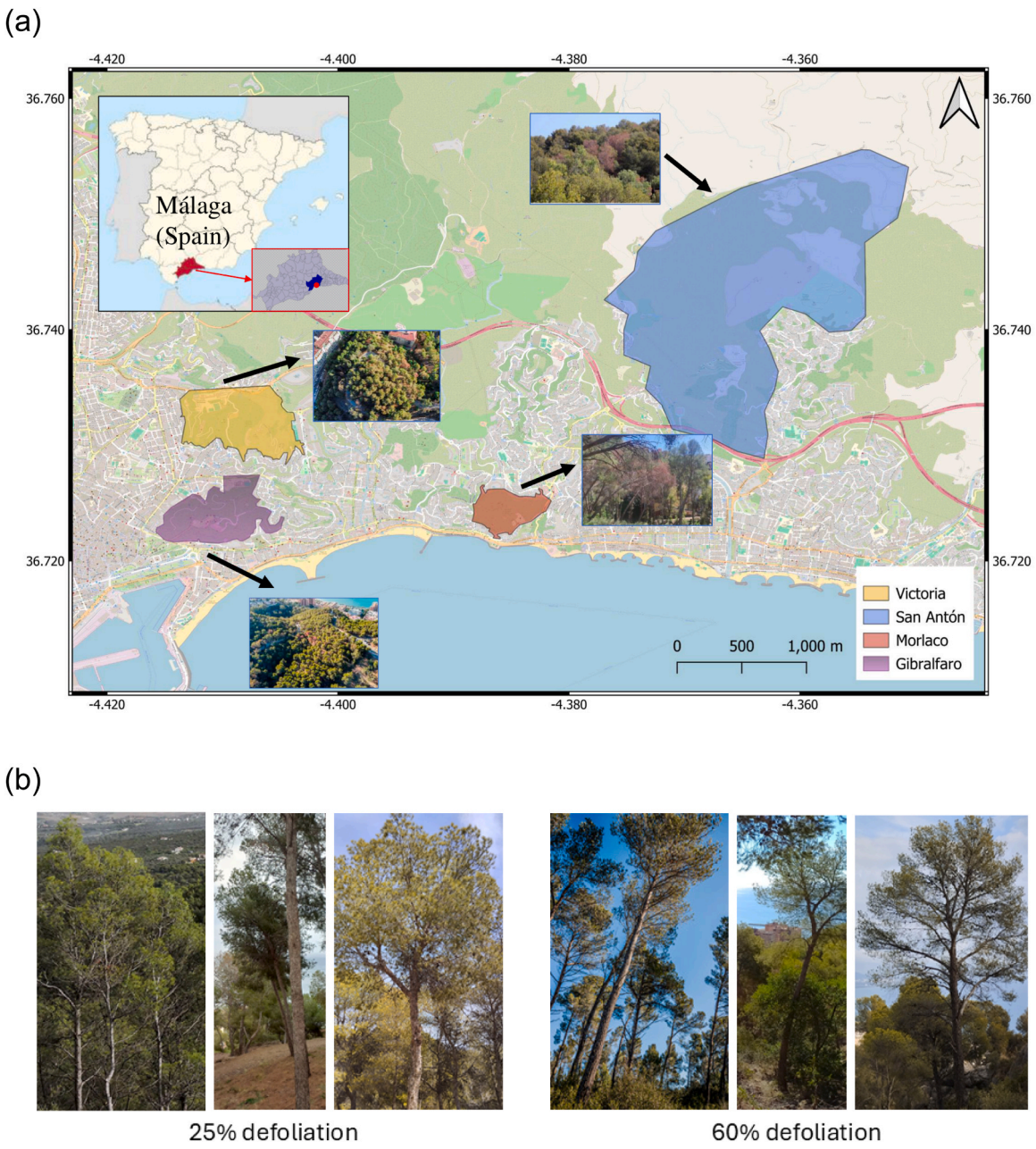



**Fig. 1.** (a) Location of the four forests sampled near the city of Málaga (inset shows the city's location in southeaster Spain), with views of affected stands. (b) View of defoliated (60 % canopy defoliation) or declining (D) trees and slightly defoliated (25 % canopy defoliation) non-declining (ND) Aleppo pine trees.

has declined (Kendall $\tau = -0.23$, $p = 0.005$; Fig. S1). From summer 2022 to winter 2023–2024, these trends culminated in extremely dry conditions driven by low rainfall and warmer temperatures; notably, winter 2021–2022 precipitation was only 30 % of the 1950–2024 average (195 mm). As a result, in late 2022 a severe drought prompted restrictions on multiple water uses in the city, including the irrigation of urban parks. This led to massive canopy dieback and elevated mortality in planted Aleppo pine stands within several parks (Fig. 1).

According to data from the Málaga meteorological station (4° 25' 11" W, 36° 43' 13" N, 80 a.s.l., period 1950–2024), climate conditions are Mediterranean with a mean annual temperature of 19.9 °C, a mean annual precipitation of 524 mm and a high potential evapotranspiration rate (879 mm) leading to a severe summer drought from May to September. The mean winter and summer temperatures are 14.6 °C and 25.9 °C, respectively, and precipitation peaks in late autumn and winter. Soils within the study sites vary from acidic to basic; however, Aleppo pine typically dominates the drier areas underlain by more basic substrates.

### 2.2. Field sampling

Sampling was done in November 2024. In each site, we selected and sampled twenty Aleppo pine trees of contrasting crown dieback. Ten trees corresponded to non-declining (hereafter ND) individuals showing defoliation levels ~ 25 % and ten trees corresponded to declining (hereafter D) individuals showing defoliation ~ 60 % (Fig. 1b). Crown defoliation was visually estimated by the first and second authors to avoid sampling bias. Randomly selected neighboring mature trees were used in the study. This protocol was repeated in north- and south-oriented slopes within each forest, thus sampling 40 trees per site and 160 trees in total.

Data on forest area and stem density were obtained from the Málaga

city Hall forest inventories. We measured tree diameter at breast height (DBH) and total height (H) of sampled trees using tapes and a Vertex IV hypsometer (Haglöf, Sweden), respectively.

To reconstruct radial growth patterns, we extracted two cores from each tree at 1.3 m using a 5-mm Pressler increment borer (Suunto, Finland). Cores were extracted perpendicular to the stem and to the maximum slope. Immediately after extraction, each core wet weight was measured using a battery-powered precision scale (Dipse TP-500), then placed in sealed tubing and carefully transported to the laboratory in a cooler to minimize moisture loss. Stem water content (SWC) was determined by drying the cores at ambient laboratory temperature for 72 h and calculating the difference between wet and dry weights.

### 2.3. Climate data, drought index and climate indices

We obtained monthly climate data (Tx, mean maximum temperature; Tn, mean minimum temperature; Pr, total precipitation) from the Málaga meteorological station (period 1950–2024). Using this climate data, we calculated the Standardized Precipitation and Evapotranspiration Index (SPEI) at monthly resolution. The SPEI was calculated using the SPEI R package (Beguería and Vicente-Serrano, 2023). The SPEI is a multiscalar drought index which is based on a cumulative water balance calculated at monthly scales (Vicente-Serrano et al., 2010). Based on previous studies (Camarero et al., 2015b), we obtained the SPEI at 1- to 24-month long scales to determine whether growth differently responded to short- and long-term droughts. The SPEI reflected the severe drought which started in winter 2021–2022 with record negative SPEI values reached in spring-summer of 2023 and 2024 (Fig. S2).

To determine the main atmospheric circulation patterns governing climate variability in the study area we obtained the North Atlantic Oscillation (NAO) index and the Western Mediterranean Oscillation (WeMO) index. The NAO is a major mode of variability of the Northern Hemisphere atmosphere mainly affecting winter conditions over Iberian (Hurrell, 1995; Rodó et al., 1997; Xoplaki et al., 2004; among others). In the western Mediterranean Basin, high NAO values are associated with dry winter conditions and reduced tree growth in spring (Camarero, 2011). The WeMO reflects the variability of rainfall precipitation in autumn and winter over the western Mediterranean basin showing negative correlations with precipitation in Eastern Spain, but potentially affecting other variables such as temperature (Martin-Vide and Lopez-Bustins, 2006). The NAO and WeMO indices were downloaded from the https://crudata.uea.ac.uk/cru/data/nao/nao.dat and https://crudata.uea.ac.uk/cru/data/moi/Web_WeMOi-2020.txt webpages, respectively.

### 2.4. Remote sensing indices

We used remote sensing data to characterize changes in tree cover and greenness through time. The Normalized Difference Vegetation Index (NDVI) measures the difference between near-infrared light, which vegetation strongly reflects, and red light, which vegetation absorbs (Wang et al., 2010). The NDVI is a good proxy of the leaf area index and the fractional vegetation cover, but the relationship between NDVI and green biomass saturates which motivated the creation of the nonlinear kernel NDVI (kNDVI) (Camps-Valls et al., 2021).

To obtain NDVI and kNDVI series we used Google Earth Engine and created image composites by integrating data from all the available Landsat-5 TM, Landsat-7 ETM+, Landsat-8 OLI and Landsat-9 OLI-2 images (White et al., 2014). Selected images were atmospherically corrected based on surface reflectance values (Zhu and Woodcock, 2012). We obtained biweekly NDVI and kNDVI series at a 30-m resolution for the period 2001–2024 using the LTR-VegChangeS application developed for extracting remote sensing data across Spain (https://landtrend.csic.es/ltr-vegchanges/; Pizarro, 2024). Then, annual means were calculated. Since Gibralfaro and Victoria forests are closely located we used the same NDVI and kNDVI series for both sites.

### 2.5. Tree-ring data

We used dendrochronology to process the wood samples (Fritts, 1976). Cores were taken to the laboratory, air dried and glued onto wooden supports. Then, they were carefully sanded with sandpapers of progressively finer grain until tree-ring boundaries were clearly visible. Samples were visually cross-dated by identifying characteristic rings common to all samples (Yamaguchi, 1991), usually being very narrow rings corresponding to known dry years such as 1986, 1995, 2000 and 2012–2013.

Tree-ring width was measured with a 0.001 mm resolution using scanned images (resolution 1200 dpi, Epson Expression 10000XL) and the CooRecorder-CDendro software (Maxwell and Larsson, 2021). The quality of cross-dating was checked using the COFECHA software, which calculates moving correlations between individual series of ring-width values and the mean sites chronologies (Holmes, 1983). To express growth as relative increases in area, we transformed the series of ring width into basal area increment (BAI) assuming concentric growth. This was done using the following formula excluding bark thickness:

$$BAI = \pi\,(r_{t-1}^2 - r_t^2) \quad (1)$$

where $r$ is the cumulative radial increment for the current ($t$) and previous ($t-1$) years. We calculated the mean BAI values for the best-replicated period (1965 −2024) also for the last 10 ($BAI_{10}$) and w0 years ($BAI_{20}$) of each individual BAI series.

The individual ring-width series were detrended by fitting cubic-smoothing spline curves of 35 years with a 50 %-frequency response cut-off. These procedures allowed preserving high-frequency variability potentially related to climate and minimized the influence of ontogeny (increase in tree size and age) or disturbance effects (Cook and Kairiukstis, 1990). Then, autoregressive models were fitted to remove the first-order autocorrelation and generate series of pre-whitened ring-width indices. Finally, a bi-weight robust mean was computed to produce mean series of growth indices for each site, orientation or vigor class. Global mean series (chronologies) for all trees and vigor classes (D and ND trees) were also built by averaging the corresponding individual indexed series.

Dendrochronological statistics were calculated over the best-replicated period including the first-order autocorrelation (AC1), mean sensitivity of ring-width indices (MS, a measure of relative changes in width between consecutive rings), mean correlation among indexed ring-width series in each site (Rbar), and the Expressed Population Signal (EPS) which is a measure of the chronology common signal (Briffa and Jones, 1990; Wigley et al., 1984). The processing of tree-ring data was done using the dplR package (Bunn, 2008; Bunn et al., 2024).

### 2.6. Statistical analyses

After checking the normality of variables using Levene-Barlett and Shapiro-Wilk and tests, respectively, we decided transforming those not fulfilling normality (log (BAI+1)). To test single effects of slope orientation, tree vigor and their interactions on several variables (DBH, SWC, BAI, $BAI_{10}$, $BAI_{20}$), analyses of variance (ANOVA) were used. Then Tukey HSD post-hoc tests were calculated to compare means of several variables (SWC, diameter, height, age, BAI, $BAI_{10}$, $BAI_{20}$) between vigor classes or between orientations within each site. To further explore the influences of orientation and tree vigor on BAI, we fitted linear mixed-effects models using the lme4 R package (Bates et al., 2015).

We calculated Pearson correlations between series of ring-width indices and monthly climate variables (Tx, Tn, Pr) to assess climate-growth relationships considering the period 1965–2024. The selected climate window spanned from previous October to current September. Similar analyses were carried out with remote sensing (period 2001–2024), teleconnection indices and the SPEI (both for the period 1965–2024). In the case of the SPEI, correlations were calculated from

**Table 2**
Comparison of variables calculated for all trees. The basal area increment (BAI) variables were calculated for the best-replicated period (1965–2024) and for the last 20 (e.g., $BAI_{20}$, period 2005–2024) and 10 years (e.g., $BAI_{10}$, period 2015–2024). Values are means ± SE for ND ($n = 40$) and D ($n = 40$) trees. Bold $t$ values indicate significant ($p \leq 0.05$) differences between the two vigour classes.

| Variable (units) | ND trees | D trees | $t$ value | $p$ |
|---|---|---|---|---|
| Diameter (cm) | 24.77 ± 0.35 | 25.18 ± 0.32 | −0.88 | 0.379 |
| Age (years) | 61 ± 1 | 61 ± 1 | 0.84 | 0.426 |
| SWC (%) | 29.52 ± 0.33 | 25.98 ± 0.45 | **6.32** | 0.001 |
| BAI ($cm^2\ yr^{-1}$) | 5.03 ± 0.23 | 6.03 ± 0. 31 | **−2.24** | 0.027 |
| BAI CV | 0.68 ± 0.01 | 0.65 ± 0.01 | 1.30 | 0.195 |
| BAI AR1 | 0.48 ± 0.01 | 0.51 ± 0.01 | 1.52 | 0.138 |
| BAI trend ($cm^2\ yr^{-2}$) | 0.05 ± 0.004 | 0.06 ± 0.005 | **−2.59** | 0.010 |
| $BAI_{20}$ ($cm^2\ yr^{-1}$) | 6.30 ± 0.26 | 7.71 ± 0.37 | **−3.10** | 0.002 |
| $BAI_{20}$ CV | 0.63 ± 0.01 | 0.60 ± 0.01 | 1.27 | 0.208 |
| $BAI_{20}$ trend ($cm^2\ yr^{-2}$) | −0.14 ± 0.02 | −0.19 ± 0.02 | 1.83 | 0.069 |
| $BAI_{10}$ ($cm^2\ yr^{-1}$) | 5.86 ± 0.31 | 7.18 ± 0.40 | **−2.19** | 0.030 |
| $BAI_{10}$ CV | 0.66 ± 0.02 | 0.67 ± 0.02 | −0.49 | 0.619 |
| $BAI_{10}$ trend ($cm^2\ yr^{-2}$) | −0.95 ± 0.04 | −1.23 ± 0.07 | **3.50** | 0.001 |

January to December and considering 1- to 24-month long scales. ANOVAs were used to compare the slopes of BAI–SPEI linear regressions between D and ND trees. All statistical analyses were performed in the R software environment (R Core Team, 2024).

We used Kendall rank correlation test (Kendall's tau (τ)) to measure the strength and direction of association between two climatic variables. This statistic varies from −1 (strong negative association) to + 1 (strong positive association). The null hypothesis ($H_0$) in a Kendall's tau test is that there is no association between the two variables (i.e., $\tau = 0$). In ANOVA tests, we estimated F-value as the ratio of variance between groups to variance within groups where a larger F-value indicates greater differences among group means. In this case, the $p$-value indicates the probability that the observed differences occurred by chance under the null hypothesis that all group means are equal where a small $p$-value (typically less than 0.05) means the differences are statistically significant, leading to rejection of the null hypothesis.

## 3. Results

### 3.1. Characteristics of ND and D trees

We did not find significant differences in tree diameter or height between D and ND trees within each site (Tables 1 and 2). Only in Gibralfaro and Victoria sites, ND trees showed higher SWC than D trees. However, differences emerged when considering terrain and vegetation factors. We found significant effects in all variables considered, namely tree diameter, SWC and BAI when they were clustered by site, orientation and tree vigor factors (Table 3, Fig. 2). The interaction between site, orientation and vigor class showed significant effects on SWC, BAI and $BAI_{20}$.

### 3.2. Patterns and changes in NDVI and kNDVI

The lowest NDVI and kNDVI values were obtained for Gibralfaro and Victoria sites mean = 0.25), whereas the highest were found in San Antón (mean = 0.18; Fig. 3). There were significant differences between the three sites' series considering NDVI ($F = 220.1$, $p < 0.001$), whereas kNDVI in San Antón was higher than in the other sites ($F = 14.9$, $p < 0.001$). We detected a noticeable drop of NDVI and particularly kNDVI in 2022. The relative decrease of kNDVI from 2021 to 2022 was 15 %. The global mean NDVI (kNDVI) values passed from 0.221 (0.029) in 2001–2021 to 0.204 (0.023) in 2022 −2024. NDVI and kNDVI series showed positive and significant correlations with the corresponding mean series of ring-width indices in five out of the eight paired correlations (Table S1). We also found that both NDVI and kNDVI increased in response to higher precipitation in the previous November and higher April minimum temperatures (Fig. S3).

### 3.3. Growth patterns

The D trees showed a significantly higher $BAI_{10}$ than ND trees in Morlaco ($p = 0.0003$), San Antón ($p = 0.0101$) and Victoria sites ($p = 0.0031$) (Tables 2 and 4). Differences between vigor classes were mediated by orientation with trees from northern orientation usually

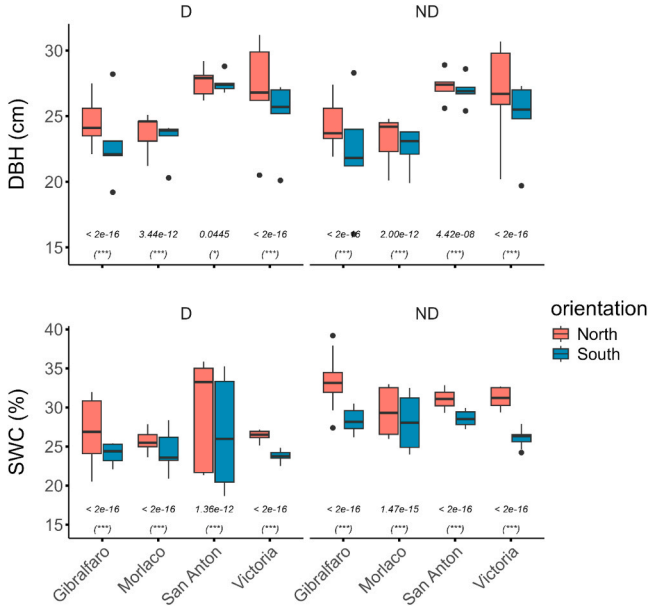



**Fig. 2.** Comparison of tree variables (Tukey HSD test) between orientations considering declining (D) and non-declining (ND) trees in the four study sites. Variables are diameter at breast height (DBH) and stem water content (SWC). The values show the significance levels of comparisons (ns, not significant; * $p \leq 0.05$; ** $0.01 \leq p < 0.05$; *** $p \leq 0.001$).

**Table 3**
Summary of ANOVAs ($F$ values) comparing several variables between sites as a function of orientation, tree vigor class and their interactions. Bold values indicate the highest $F$ value for each variable. Variables' abbreviations: DBH, diameter at breast height; SWC, stem water content; BAI, log-transformed basal area increment; $BAI_{10}$ and $BAI_{20}$, mean log-transformed BAI values for the last 10 and 20 years, respectively. Significance levels: *$p \leq 0.05$, ** $0.01 \leq p < 0.05$, *** $0.01 < p$.

| Factor | Variable | | | | |
|---|---|---|---|---|---|
| | DBH | SWC | BAI | $BAI_{10}$ | $BAI_{20}$ |
| Site (S) | **1891.96***** | 317.71*** | **759.83***** | **201.54***** | **262.55***** |
| Orientation (O) | 615.01*** | 2578.41*** | 299.46*** | 40.18*** | 131.71*** |
| Vigor (V) | 83.58*** | **3771.06***** | 118.57*** | 13.96*** | 45.84*** |
| S × O | 87.67*** | 122.06*** | 66.86*** | 15.92*** | 18.59*** |
| S × V | 4.65* | 155.40*** | 37.59*** | 7.36*** | 16.02*** |
| O × V | 3.67 | 84.13*** | 8.04*** | 3.05* | 7.44*** |
| S × O × V | 1.69 | 33.49*** | 6.22*** | 2.71 | 4.41*** |

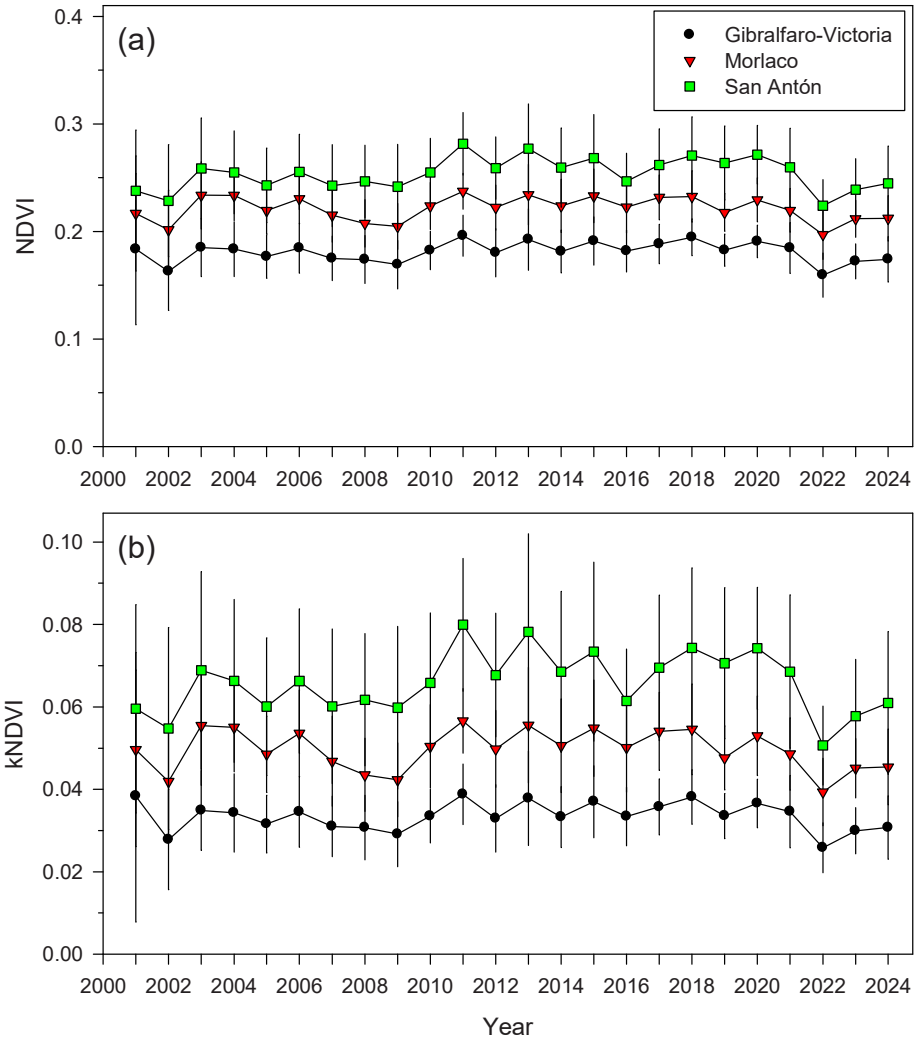



**Fig. 3.** Annual mean values of (a) NDVI and (b) kNDVI obtained for the study sites. Values are means ± SD.

**Table 4**
Tree-ring width statistics of the sampled trees calculated for non-declining (ND) and declining (D) trees. Values are means (standard deviation) and considering the common 1965–2024 period excepting for $BAI_{20}$. Abbreviations: $BAI_{20}$, basal area increment in the last 20 years; Rbar, mean correlation between trees; AC1, first-order autocorrelation coefficient; MS, mean sensitivity of ring-width indices; EPS, Expressed Population Signal. Different letters indicate significant ($p < 0.05$) differences of $BAI_{20}$ between plots according to Tukey HSD tests.

| Site | Orientation | Vigor class | Plot | No trees | $BAI_{20}$ ($cm^2\ yr^{-1}$) | Rbar | AC1 | MS | EPS |
|---|---|---|---|---|---|---|---|---|---|
| Gibralfaro | North | ND | GNND | 10 | 5.21 (4.00)a | 0.42 | 0.52 | 0.46 | 0.88 |
| | | D | GND | 10 | 4.22 (2.95)a | 0.43 | 0.69 | 0.41 | 0.88 |
| | South | ND | GSND | 10 | 4.30 (2.97)a | 0.37 | 0.65 | 0.40 | 0.86 |
| | | D | GSD | 10 | 4.61 (3.77)a | 0.53 | 0.69 | 0.42 | 0.92 |
| Morlaco | North | ND | MNND | 10 | 8.30 (5.41)c | 0.50 | 0.65 | 0.42 | 0.91 |
| | | D | MND | 10 | 10.70 (6.71)d | 0.46 | 0.65 | 0.40 | 0.89 |
| | South | ND | MSND | 10 | 5.91 (4.67)b | 0.54 | 0.66 | 0.50 | 0.92 |
| | | D | MSD | 10 | 7.41 (5.75)c | 0.50 | 0.66 | 0.50 | 0.91 |
| San Antón | North | ND | SNND | 10 | 9.78 (4.40)c | 0.69 | 0.82 | 0.34 | 0.95 |
| | | D | SND | 10 | 11.20 (5.40)d | 0.67 | 0.81 | 0.34 | 0.95 |
| | South | ND | SSND | 10 | 6.88 (3.68)c | 0.69 | 0.82 | 0.40 | 0.95 |
| | | D | SSD | 10 | 10.83 (5.19)d | 0.66 | 0.81 | 0.36 | 0.95 |
| Victoria | North | ND | VNND | 10 | 5.82 (4.57)b | 0.43 | 0.58 | 0.44 | 0.88 |
| | | D | VND | 10 | 7.61 (5.42)c | 0.38 | 0.55 | 0.42 | 0.87 |
| | South | ND | VSND | 10 | 3.78 (2.84)a | 0.40 | 0.58 | 0.39 | 0.88 |
| | | D | VSD | 10 | 4.80 (3.39)a | 0.37 | 0.79 | 0.55 | 0.86 |

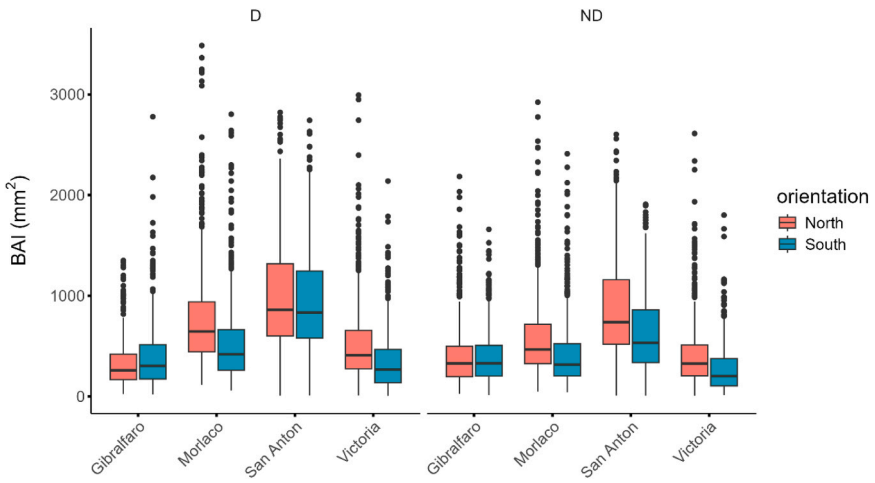



**Fig. 4.** Comparison of basal area increment (bai, in $mm^2\ yr^{-1}$) between orientations considering declining (D) and non-declining (ND) trees in the four study sites. BAI values correspond to the last measured 10 years, i.e. $BAI_{10}$.

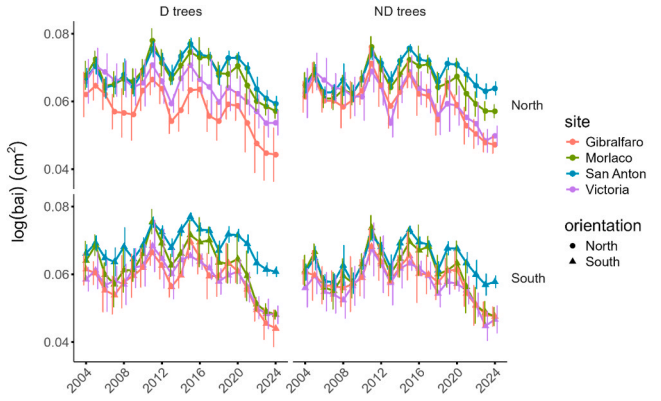



**Fig. 5.** Comparison of basal area increment (bai, log-transformed data) between orientations considering declining (D) and non-declining (ND) trees in the four study sites. Plots show log-transformed bai data for the period 2004–2024. Values are means ± SD.

growing more than trees from southern orientation (Table 3, Figs. 4 and 5).

Globally, D trees grew more than ND trees, but this difference reversed in the period 2022–2024, when a severe winter drought occurred (Fig. 6). At tree level, tree diameter was positively and significantly correlated with mean BAI in D trees, but negatively related to the BAI coefficient of variation (Fig. S4). However, BAI was positively correlated with the BAI first-order autocorrelation in the case of ND trees

### 3.4. Growth responses to climate variability and drought severity

Tree growth was enhanced by high precipitation in the previous December and high minimum temperatures in the current April (Fig. 7). In contrast, long winter droughts constrained growth with correlations between ring-width indices and the SPEI peaking for 17-month January SPEI values ($r = 0.473$).

BAI increased as SPEI did in all sites, although their correlation coefficients differed, being highest in San Antón and lowest in Victoria (Fig. S5). There were no significant differences between ND and D trees in the slopes of the linear regressions fitted to BAI-SPEI relationships.

The December temperature and the April temperature were negatively correlated with December NAO and April WeMO indices, respectively (Fig. S6). Regarding NAO values, only the February index showed a significant positive trend (slope = 0.032, $r = 0.28$, $p = 0.03$), which suggests conditions in late winter are becoming drier. In fact, the 17-month January SPEI showed a significant negative trend ($\tau = -0.297$, $p = 0.021$) confirming winter aridification.

The series of ring-width indices and December-January WeMO were negatively related ($r = -0.30$, $p = 0.025$; Fig. S7). However, this relationship was unstable through time being significant from the late 1970s to the early 2000s.

## 4. Discussion

The recent die-off episode affecting the study urban Aleppo pine forests was attributed to a prolonged drought event characterized by an unusually dry winter. The drought episode started three years before observing the abrupt reduction in growth, whose effect was evidenced one year before the decline in tree cover and greenness. This shows the temporal decoupling between primary (canopy cover) and secondary (tree-ring width) growth. Despite such temporal disconnection, remotely sensed data and growth observations were spatially associated, being the sites with highest (San Antón) or lowest growth rates (Gibralfaro, Victoria) strongly linked to those with highest or lowest NDVI or kNDVI values. Correlations between annual NDVI or kNDVI and indexed ring-width series peaked in the fast-growing site. The latter showed similar responses to climate variability.

Overall, wet conditions in the prior autumn and winter and warm spring conditions enhanced growth and canopy cover, whereas long dry conditions during winter triggered growth decline. The die-off was attributed to extremely warm-dry conditions in autumn and winter associated to a positive phase of the NAO. The observed long-term dry winter over the western Mediterranean is linked to a weakening of Atlantic Ocean poleward heat transport leading to persistent atmospheric anticyclone in this hot spot (Delworth et al., 2022). Moreover, these authors argue that the inertia of atmospheric circulation patterns hampers a full recovery of winter rainfall over the western Mediterranean basin during this century even if substantial climate mitigation efforts are achieved. Therefore, managers of urban forests in this region should consider such drying and persistent climate scenario even for drought-tolerant tree species.

Regional influences related to atmospheric patterns (NAO, WeMO) and climate variability (drought) differently impacted the study forests depending on local conditions (site, orientation) and tree features (growth rate, SWC). Trees in wet-cool north-oriented slopes showed higher growth rates than those in warm-dry south-oriented slopes. Site and orientation were more important drivers of growth than vigor, emphasizing the locally contingent influences on wood formation including microclimate, soil conditions and tree-to-tree competition

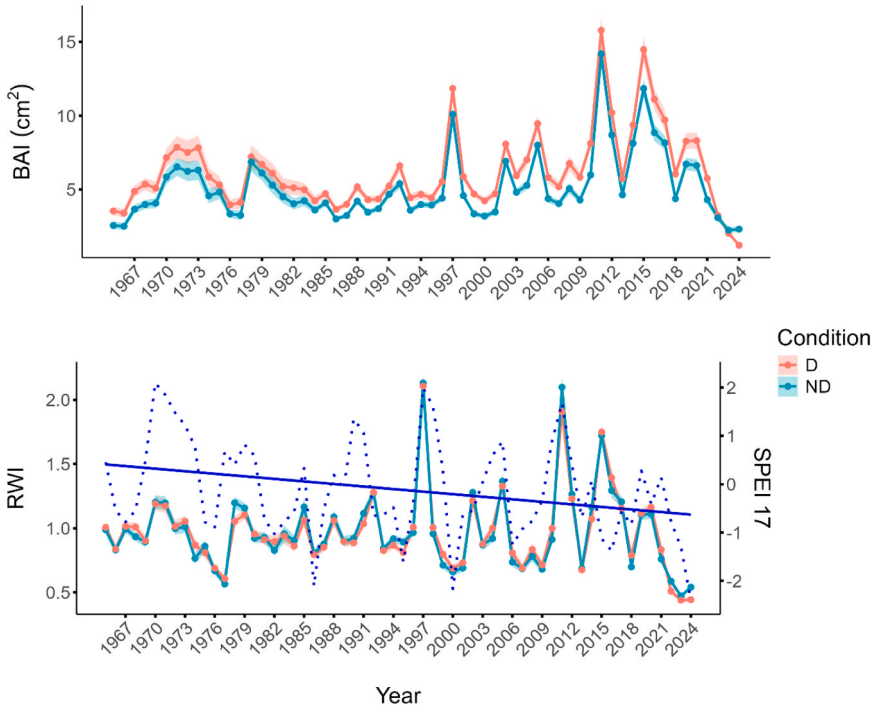



**Fig. 6.** (a) Basal area increment values of non-declining (ND) and declining (D) trees. (b) Series of ring-width indices of the two vigor classes and 17-month January SPEI (dotted blue line and regression, right y axis). The SPEI scale was selected because it showed the highest correlation with growth indices. Values are means ± SE.

(Sergent et al., 2014; Gazol et al., 2017; Jiang et al., 2019; Isaacson et al., 2023). For instance, several oak species present a rapid post-drought recovery in urban (Gillner et al., 2013) and natural forests (Anderegg et al. 2015), but their remarkable resilience depends on site growing conditions (Dervishi et al., 2022).

It would be expected that competition for soil water and nutrients would be higher in dense stands leading to lower growth rates and die-off as it has been found before in similar natural and planted Aleppo pine stands (Camarero et al., 2015a; Sánchez-Salguero et al. 2012; Manrique-Alba et al., 2020). Unexpectedly, in our case, those most affected trees by the recent drought showed higher growth rates in the past. This prodigal water-use behavior of declining trees has been observed before in Scots pine (*Pinus sylvestris* L.) suggesting that fast-growing trees forming wider xylem conduits and showing higher capacity to uptake soil water were predisposed to drought damage when conditions turned extremely dry (Voltas et al., 2013). Stem water content was lower in declining trees indicating a lower sapwood hydraulic capacitance. In other words, declining trees were hydraulically underbuilt for tolerating dry conditions. This idea could be further tested using retrospective measurements of wood anatomy and wood isotope composition ($\delta^{13}C$, $\delta^{18}O$) (Esperon-Rodriguez et al., 2020; Locosselli et al., 2024), that could provide further understanding of drought responses (Pellizzari et al., 2016). Changes in tree-ring wood $\delta^{15}N$ could be also measured in areas exposed to elevated NOx traffic emissions to investigate drought-pollution interactive impacts on urban forests (Saurer et al., 2004; Battipaglia et al., 2010). However, this pollution source does not seem to impact growth resistance to drought in urban forests situated far from traffic sources such as highways (Hirsch et al., 2023), as it was our case. Lastly, bark, leaf and wood concentrations of trace elements, particularly heavy metals related to air pollution (e.g., Cr, Pb, Zn), could be tracked to research the impacts of pollution on drought-stressed trees (Batkhuyag et al., 2023).

A limitation of our approach is that we lacked precise historical information on past management disturbances (thinning, logging) and on current stand structure or soil conditions. Other studies have also emphasized the importance of site conditions for tree growth in plantations (Li et al., 2024) Nevertheless, the study tree-ring series did not show clearly releases associated to past thinning and competition was not considered a major driver of growth recovery after drought according to a recent meta-analysis (Castagneri et al., 2022). However, in Helsinki urban forests, the decline and mortality of Scots pine trees were attributed to tree-to-tree competition and successive droughts which predisposed and triggered die-off, respectively (Helama et al., 2012).Our results concur with previous analyses demonstrating the importance of thinning and adaptive silviculture to manage dense, drought-stressed stands under semi-arid climate conditions (Navarro-Cerrillo et al., 2018, 2023; Cachinero-Vivar et al., 2021, 2024)). Moreover, managers should carefully plan thinning regimes considering drought severity and frequency in similar seasonally dry cities and urban areas dominated by drought-avoiding species such as Aleppo pine (Manrique-Alba et al., 2022).

## 5. Conclusion

We characterized a drought-induced forest die-off episode differently affecting four urban forests. Site and orientation played important roles conditioning the impacts of a severe, long winter drought. Regarding tree features, declining trees grew more in the past and presented lower stem water content. These two characteristics could be further explored as early-warning signals of impeding dieback and tree death. Adaptive urban silviculture could thin dense stands to alleviate competition for soil water, although this may be a transitory measure. Long-term managements of die-off in urban forests dominated by drought-tolerant tree species may consider replacing them by tree and shrub species showing a much higher drought tolerance and better resisting current drying conditions such as Mediterranean junipers or broadleaves.

## CRediT authorship contribution statement

**Antonio M. Cachinero-Vivar:** Writing – review & editing, Visualization, Software, Resources, Methodology, Investigation, Funding acquisition, Formal analysis, Data curation, Conceptualization. **Oscar**

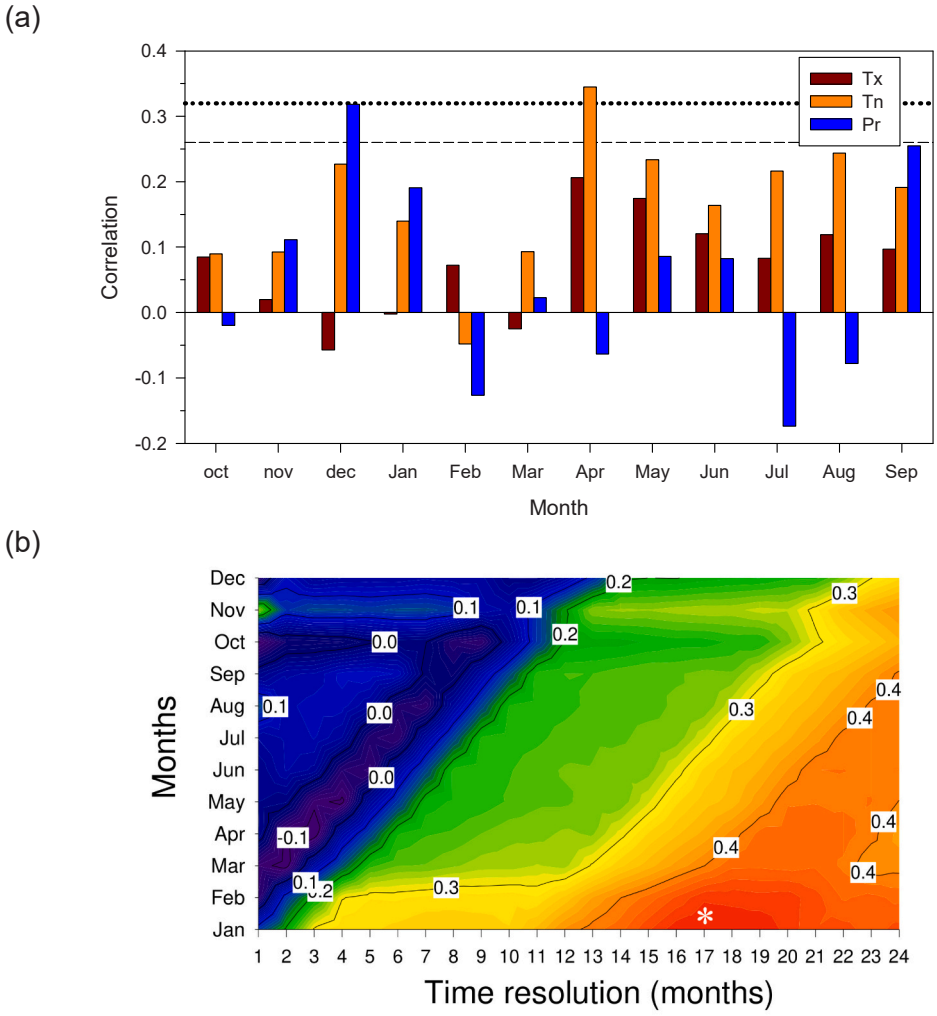



**Fig. 7.** (a) Climate- and (b) drought-growth relationships. In plot (a), bars are Pearson correlations calculated between monthly climate variables (Tx, mean maximum temperature; Tn, mean maximum temperature; Pr, total precipitation) and annual ring-width indices. Correlations were calculated from the prior (months abbreviated by lowercase letters) to current (months abbreviated by uppercase letters) years. Dashed and dotted horizontal lines show the 0.05 and 0.01 significance levels, respectively. In plot (b), the color scale shows correlations between the monthly SPEI drought index and ring-width indices. Correlations were calculated for 1- to 24-long monthly scales (x axis). The asterisk in plot (b) shows the time scale and month where the maximum correlation was found (17 months, January).

**Pérez-Priego:** Writing – review & editing, Visualization, Validation, Supervision, Investigation, Funding acquisition, Formal analysis, Data curation, Conceptualization. **J. Julio Camarero:** Writing – original draft, Visualization, Validation, Software, Resources, Project administration, Methodology, Investigation, Funding acquisition, Formal analysis, Data curation, Conceptualization.

## Funding sources

J.J.C. thanks the support of the Science and Innovation Ministry of Spain (projects PID2021-123675OB-C43 and TED2021-129770B-C21). We also acknowledge the support of project REMEDIO (PID2021-128463OB-I00).

## State

During the preparation of this work, authors did not use any AI tool.

## Declaration of Competing Interest

Authors declare no competing interests.

## Acknowledgments

We thank the Málaga town hall for their collaboration and help during sampling.

## Appendix A. Supporting information

Supplementary data associated with this article can be found in the online version at doi:10.1016/j.ufug.2025.128970.

## References

Anderegg, W.R.L., Schwalm, C., Biondi, F., Camarero, J.J., Koch, G., Litvak, M., Ogle, K., Shaw, J.D., Shevliakova, E., Williams, A.P., Wolf, A., Ziaco, E., Pacala, S., 2015. Pervasive drought legacies in forest ecosystems and their implications for carbon cycle models. Science 349, 528–532.

Bates, D., Mächler, M., Bolker, B., Walker, S., 2015. Fitting linear mixed-effects models using lme4. J. Stat. Soft 67, 1–48. https://doi.org/10.18637/jss.v067.i01.

Batkhuyag, E., Lehmann, M.M., Cherubini, P., Ulziibat, B., Soyol-Erdene, T., Schaub, M., Saurer, M., 2023. Combination of multiple stable isotope and elemental analyses in urban trees reveals air pollution and climate change effects in Central Mongolia. Ecol. Indic. 154, 110719.

Battipaglia, G., Marzaioli, F., Lubritto, C., Altieri, S., Strumia, S., Cherubini, P., Cotrufo, M.F., 2010. Traffic pollution affects tree-ring width and isotopic composition of *Pinus pinea*. Sci. Total Environ. 408, 586–593.

Beguería, S., Vicente-Serrano, S.M., 2023. SPEI: Calculation of the Standardized Precipitation-Evapotranspiration Index. ⟨https://github.com/sbegueria/SPEI⟩.
Bialecki, M.B., Fahey, R.T., Scharenbroch, B., 2018. Variation in urban forest productivity and response to extreme drought across a large metropolitan region. Urban Ecoyst. 12, 157–169.
Bowler, D.E., Buyung-Ali, L., Knight, T.M., Pullin, A.S., 2010. Urban greening to cool towns and cities: a systematic review of the empirical evidence. Land. Urban Plan 97, 147–155. https://doi.org/10.1016/j.landurbplan.2010.05.006.
Briffa, K.R., Jones, P.D., 1990. Basic chronology statistics and assessment. In: Cook, E.R., Kairiukstis, L.A. (Eds.), Methods of Dendrochronology. Applications in the Environmental Sciences. Kluwer Academic Publishers, Dordrecht, pp. 137–152.
Bunn, A.G., 2008. A dendrochronology program library in R (dplR). Dendrochronologia 26, 115–124. https://doi.org/10.1016/j.dendro.2008.01.002.
Bunn A., Korpela M., Biondi F., Campelo F., Klesse S., Mérian P., Qeadan F., Zang C. 2024. dplR: Dendrochronology Program Library in R. R package version 1.7.8, ⟨https://CRAN.R-project.org/package=dplR⟩.
Cachinero-Vivar, A.M., Navarro-Cerrillo, R.M., Cabrera-Puerto, R.J., Pérez-Priego, O., 2024. Impact of thinning on leaf economics, plant hydraulics, and growth dynamics. For. Ecol. Manag. 562, 121914.
Cachinero-Vivar, A.M., Palacios-Rodríguez, G., Lara-Gómez, M.A., Navarro-Cerrillo, R. M., 2021. Thinning effect of C sequestration along an elevation gradient of Mediterranean Pinus spp. plantations. Forests 12 (11), 1583.
Camarero, J.J., 2011. Direct and indirect effects of the North Atlantic Oscillation on tree growth and forest decline in Northeastern Spain. In: Vicente-Serrano, S.M., Trigo, R. M. (Eds.), Hydrological, Socioeconomic and Ecological Impacts of the North Atlantic Oscillation in the Mediterranean Region. Advances in Global Change Research. Springer, pp. 129–152.
Camarero, J.J., Gazol, A., Sangüesa-Barreda, G., Oliva, J., Vicente-Serrano, S.M., 2015a. To die or not to die: early-warning signals of dieback in response to a severe drought. J. Ecol. 103, 44–57.
Camarero, J.J., Gazol, A., Tardif, J.C., Conciatori, F., 2015b. Attributing forest responses to global-change drivers: limited evidence of a $CO_2$-fertilization effect in Iberian pine growth. J. Biogeogr. 42, 2220–2233.
Camps-Valls, G., Campos-Taberner, M., Moreno-Martínez, A., Walther, S., Duveiller, G., Cescatti, A., Mahecha, M., Muñoz-Marí, J., García-Haro, F.J., Guanter, L., Gamon, J., Jung, M., Reichstein, M., Running, S.W., 2021. A unified vegetation index for quantifying the terrestrial biosphere. Sci. Adv. 7, eabc7447. https://doi.org/10.1126/sciadv.abc7447.
Castagneri, D., Vacchiano, G., Hacket-Pain, A., DeRose, R.J., Klein, T., Bottero, A., 2022. Meta-analysis reveals different competition effects on tree growth resistance and resilience to drought. Ecosystems 25, 30–43.
Chen, Z., Hem, X., Cook, E.R., He, H., Chen, W., Sun, Y., Cui, M., 2011. Detecting dryness and wetness signals from the tree rings in Shenyang, Northeast China. Paleogeogr. Paleoclimatol. Paleoecol. 302, 301–310.
Cramer, W., Guiot, J., Fader, M., Garrabou, J., Gattuso, J.-P., Iglesias, A., Lange, M.A., Lionello, P., Llasat, M.C., Paz, S., 2018. Climate change and interconnected risks to sustainable development in the Mediterranean. Nat. Clim. Change 8, 972–980.
Czaja, M., Kołton, A., Muras, P., 2020. The complex issue of urban trees-stress factor accumulation and ecological service possibilities. Forests 11, 932.
David, A., Boura, A., Kraepiel, Y., Lata, J.-C., Barot, S., Abbadie, L., Ngao, J., 2015. Long Term Impact of Climate on Tree-growth Patterns in Paris Street Trees and Its Consequences on Tree Cooling Potential: A Dendroclimatic Approach. Conference Paper, ICUC9.
Delworth, T.L., Cooke, W.F., Naik, V., Paynter, D., Zhang, L., 2022. A weakened AMOC may prolong greenhouse gas-induced Mediterranean drying even with significant and rapid climate change mitigation. Proc. Natl. Acad. Sci. USA 119, e2116655119. https://doi.org/10.1073/pnas.2116655119 (2022).
Dervishi, V., Poschenrieder, W., Rötzer, T., Moser-Reischl, A., Pretzsch, H., 2022. Effects of climate and drought on stem diameter growth of urban tree species. Forests 13, 641. https://doi.org/10.3390/f13050641.
Esperon-Rodriguez, M., Rymer, P.D., Power, S.A., Challis, A., Marchin, R.M., Tjoelker, M. G., 2020. Functional adaptations and trait plasticity of urban trees along a climatic gradient. Urban For. Urban Green. 54, 126771.
Esperon-Rodriguez, M., Tjoelker, M.G., Lenoir, J., Baumgartner, J.B., Beaumont, L.J., Nipperess, D.A., et al., 2022. Climate change increases global risk to urban forests. Nat. Clim. Chang 12, 950–955. https://doi.org/10.1038/s41558-022-01465-8.
Farrell, C., Szota, C., Arndt, S.K., 2015. Urban plantings: 'living laboratories' for climate change response. Trends Plant Sci. 20, 597–599. https://doi.org/10.1016/j.tplants.2015.08.006.
Franceschi, E., Moser-Reischl, A., Honold, M., Rahman, M.A., Pretzsch, H., Pauleit, S., Rötzer, T., 2023. Urban environment, drought events and climate change strongly affect the growth of common urban tree species in a temperate city. Urban For. Urban Green. 88, 128083. https://doi.org/10.1016/j.ufug.2023.128083.
Fritts, H.C., 1976. Tree Rings and Climate. Academic Press, London.
García de la Serrana, R., Vilagrosa, A., Alloza, J.A., 2015. Pine mortality in Southeast Spain after an extreme dry and warm year: Interactions among drought stress, carbohydrates and bark beetle attack. Trees - Struct. Funct. 29, 1791–1804. https://doi.org/10.1007/s00468-015-1261-9.
Gazol, A., Camarero, J.J., Anderegg, W.R.L., Vicente-Serrano, S.M., 2017. Impacts of droughts on the growth resilience of northern hemisphere forests. Glob. Ecol. Biogeogr. 26, 166–176. https://doi.org/10.1111/geb.12526.
Gillner, S., Bräuning, A., Roloff, A., 2014. Dendrochronological analysis of urban trees: climatic response and impact of drought on frequently used tree species. Trees Struct. Funct. 28, 1079–1093. https://doi.org/10.1007/s00468-014-1019-9.
Gillner, S., Vogt, J., Roloff, A., 2013. Climatic response and impacts of drought on oaks at urban and forest sites. Urban. For. Urban. Green. 12, 597–605. https://doi.org/10.1016/j.ufug.2013.05.003.
Gregg, J.W., Jones, C.G., Dawson, T.E., 2003. Urbanization effects on tree growth in the vicinity of New York City. Nature 424, 183–187. https://doi.org/10.1038/nature01728.
Grossiord, C., Buckley, T.N., Cernusak, L.A., Novick, K.A., Poulter, B., Siegwolf, R.T.W., Sperry, J.S., McDowell, N.G., 2020. Plant responses to rising vapor pressure deficit. New Phytol. 226, 1550–1566. https://doi.org/10.1111/nph.164852020.
Hammond, W.M., Williams, A.P., Abatzoglou, J.T., Adams, H.D., Klein, T., López, R., Sáenz-Romero, C., Hartmann, H., Breshears, D.D., Allen, C.D., 2022. Global field observations of tree die-off reveal hotter-drought fingerprint for Earth's forests. Nat. Commun. 13, 1761.
Helama, S., Läänelaid, A., Raisio, J., Tuomenvirta, H., 2012. Mortality of urban pines in Helsinki explored using tree rings and climate records. Trees Struct. Funct. 26, 353–362. https://doi.org/10.1007/s00468-011-0597-z.
Hibbard, K.A., Hoffman, F.M., Huntzinger, D., West, T.O., 2017. Changes in land cover and terrestrial biogeochemistry. In: Wuebbles, D.J., Fahey, D.W., Hibbard, K.A., Dokken, D.J., Stewart, B.C., Maycock, T.K. (Eds.), Climate Science Special Report: Fourth National Climate Assessment, I. U.S. Global Change Research Program, Washington, DC, pp. 277–302. https://doi.org/10.7930/J0416V6X.
Hirsch, M., Böddeker, H., Albrecht, A., Saha, S., 2023. Drought tolerance differs between urban tree species but is not affected by the intensity of traffic pollution. Trees Struct. Funct. 37, 111–131.
Holmes, R.L., 1983. Computer-assisted quality control in tree-ring dating and measurement. Tree-Ring Bull. 43, 69–78.
Huang, K., Li, X., Liu, X., Seto, K.C., 2019. Projecting global urban land expansion and heat island intensification through 2050. Environ. Res. Lett. 14, 114037. https://doi.org/10.1088/1748-9326/ab4b71.
Hurrell, J.W., 1995. Decadal trends in the North Atlantic Oscillation and relationships to regional temperature and precipitation. Science 269, 676–679.
Isaacson, B.N., Yang, Y., Anderson, M.C., Clark, K.L., Grabosky, J.C., 2023. The effects of forest composition and management on evapotranspiration in the New Jersey Pinelands. Agric. For. Meteor. 339, 109588. https://doi.org/10.1016/j.agrformet.2023.109588.
Jiang, P., Liu, H., Piao, S., Ciais, P., Wu, X., Yin, Y., Wang, H., 2019. Enhanced growth after extreme wetness compensates for post-drought carbon loss in dry forests. Nat. Comm. 10, 195. https://doi.org/10.1038/s41467-018-08229-z.
Cook, E.R., Kairiukstis, L.A. (Eds.), 1990. Methods of Dendrochronology: Applications in the Environmental Sciences. Kluwer Academic Publishers, Dordrecht, The Netherlands, p. 394.
Leuzinger, S., Vogt, R., Körner, C., 2010. Tree surface temperature in an urban environment. Agric. Meteor. 150, 56–62. https://doi.org/10.1016/j.agrformet.2009.08.006.
Li, D., Liao, W., Rigden, A.J., Liu, X., Wang, D., Malyshev, S., Shevliakova, E., 2019. Urban heat island: Aerodynamics or imperviousness? Sci. Adv. 5, eaau4299. https://doi.org/10.1126/sciadv.aau4299.
Li, J., Xie, Y., Camarero, J.J., Gazol, A., González de Andrés, E., Ying, L., Shen, Z., 2024. Optimistic growth of marginal region plantations under climate warming: assessing divergent drought resilience. Glob. Change Biol. 30, e17459.
Liu, Z., Zhan, W., Bechtel, B., Voogt, J., Lai, J., Chakraborty, T., Wang, Z.-H., Li, M., Huang, F., Lee, X., 2022. Surface warming in global cities is substantially more rapid than in rural background areas. Commun. Earth Environ. 3, 219. https://doi.org/10.1038/s43247-022-00539-x.
Locosselli, G.M., Cintra, B.L.B., Ferreira, L.S., Da Silva-Luz, C.L., Miyahara, A.A.L., Brienen, R.J.W., Gloor, E., Bloom, A., Grandis, A., Buckeridge, M.S., 2024. Stress-tolerant trees for resilient cities: tree-ring analysis reveals species suitable for a future climate. Urban Clim. 55, 101964. https://doi.org/10.1016/j.uclim.2024.101964.
Maestre, F.T., Cortina, J., 2004. Are *Pinus halepensis* plantations useful as a restoration tool in semiarid Mediterranean areas? For. Ecol. Manag. 198, 303–317. https://doi.org/10.1016/j.foreco.2004.05.040.
Manrique-Alba, A., Beguería, S., Camarero, J.J., 2022. Long-term effects of forest management on post-drought growth resilience: an analytical framework. Sci. Tot. Environ. 810, 152374.
Manrique-Alba, A., Beguería, S., Molina, A.J., González-Sanchis, M., Tomàs-Burguera, M., del Campo, A.D., Colangelo, M., Camarero, J.J., 2020. Long-term thinning effects on tree growth, drought response and water use efficiency at two Aleppo pine plantations in Spain. Sci. Tot. Environ. 728, 138536.
Marchin, R.M., Esperon-Rodriguez, M., Tjoelker, M.G., Ellsworth, D.S., 2022. Crown dieback and mortality of urban trees linked to heatwaves during extreme drought. Sci. Tot. Environ. 850, 157915. https://doi.org/10.1016/j.scitotenv.2022.157915.
Martin-Vide, J., Lopez-Bustins, J.A., 2006. The Western Mediterranean Oscillation and rainfall in the Iberian Peninsula. Int. J. Clim. 26, 1455–1475. https://doi.org/10.1002/joc.1388.
Maxwell, R.S., Larsson, L.-A., 2021. Measuring tree-ring widths using the CooRecorder software application. Dendrochronologia 67, 125841.
Miyahara, A.A.L., Wild, T., Sandre, A.A., Pellegrino, P.R.M., Filho, C.A.S., Buckeridge, M. S., Locosselli, G.M., 2022. Developing and classifying urban biomes as a basis for nature-based solutions. Urban Clim. 45, 101251.
Morcillo, L., Muñoz-Rengifo, J.C., Torres-Ruiz, J.M., Delzon, S., Moutahir, H., Vilagrosa, A., 2022. Post-drought conditions and hydraulic dysfunction determine tree resilience and mortality across Mediterranean Aleppo pine (*Pinus halepensis*) populations after an extreme drought event. Tree Physiol. 42, 1364–1376. https://doi.org/10.1093/treephys/tpac001.

Moser, A., Rötzer, T., Pauleit, S., Pretzsch, H., 2016. The urban environment can modify drought stress of small-leaved lime (*Tilia cordata* Mill.) and black locust (*Robinia pseudoacacia* L.). Forests 7 (3). https://doi.org/10.3390/f7030071.

Navarro-Cerrillo, R.M., Cachinero-Vivar, A.M., Pérez-Priego, Ó., Aspizua Cantón, R., Begueria, S., Camarero, J.J., 2023. Developing alternatives to adaptive silviculture: Thinning and tree growth resistance to drought in a Pinus species on an elevated gradient in Southern Spain. For. Ecol. Manag. 537, 120936. https://doi.org/10.1016/j.foreco.2023.120936.

Navarro-Cerrillo, R.M., Sánchez-Salguero, R., Rodríguez, C., Duque, J., Moreno-Rojas, J. M., Palacios-Rodríguez, G., Camarero, J.J., 2018. Is thinning an alternative when trees could die in response to drought? The case of planted *Pinus nigra* and *P. sylvestris* stands in southern Spain. For. Ecol. Manag. 433, 313–324.

Pataki, D.E., McCarthy, H.R., Litvak, E., Pincetl, S., 2011. Transpiration of urban forests in the Los Angeles metropolitan area. Ecol. Appl. 21, 661–677.

Pellizzari, E., Camarero, J.J., Gazol, A., Sangüesa-Barreda, G., Carrer, M., 2016. Wood anatomy and carbon-isotope discrimination support long-term hydraulic deterioration as a major cause of drought-induced dieback. Glob. Change Biol. 22 (6), 2125–2137.

Pizarro, M., 2024. LandTrendr-based Vegetation Changes in Spain (1984−present). Inst. Piren. Ecol. (IPECSIC). https://doi.org/10.20350/digitalCSIC/16457.

Pretzsch, H., Biber, P., Uhl, E., Dahlhausen, J., Schütze, G., Perkins, D., Rötzer, T., Caldentey, J., Koike, T., Con, T.V., Chavanne, A., Toit, B.D., Foster, K., Lefer, B., 2017. Climate change accelerates growth of urban trees in metropolises worldwide. Sci. Rep. 7, 15403. https://doi.org/10.1038/s41598-017-14831-w.

R Core Team, 2024. R: A Language and Environment for Statistical Computing. R Foundation, Vienna, Austria. ⟨https://www.R-project.org/⟩.

Rakoto, P.Y., Deilami, K., Hurley, J., Amati, M., Sun, Q.C., 2021. Revisiting the cooling effects of urban greening: Planning implications of vegetation types and spatial configuration. Urban For. Urban Green. 64, 127266.

Rodó, X., Baert, E., Comín, F., 1997. Variations in the seasonal rainfall in Southern Europe during the present century: Relationship with the North Atlantic Oscillation and the El Niño–Southern Oscillation. Clim. Dynam. 13, 275–284. https://doi.org/10.1007/s003820050165.

Rötzer, T., Moser-Reischl, A., Rahman, M.A., Hartmann, C., Paeth, H., Pauleit, S., Pretzsch, H., 2021. Urban tree growth and ecosystem services under extreme drought. Agric. For. Meteor. 308−309, 108532.

Roy, S., Byrne, J., Pickering, C., 2012. A systematic quantitative review of urban tree benefits, costs, and assessment methods across cities in different climatic zones. Urban For. Urban Green. 11, 351–363. https://doi.org/10.1016/j.ufug.2012.06.006.

Sánchez-Salguero, R., Navarro-Cerillo, R.M., Camarero, J.J., Fernández-Cancio, A., 2012. Selective drought-induced decline of pine species in southeastern Spain. Clim. Change 113, 767–785.

Saurer, M., Cherubini, P., Ammann, M., De Cinti, B., Siegwolf, R., 2004. First detection of nitrogen from NOx in tree rings: a $^{15}N/^{14}N$ study near a motorway. Atmos. Environ. 38, 2779–2787.

Sergent, A.S., Rozenberg, P., Bréda, N., 2014. Douglas-fir is vulnerable to exceptional and recurrent drought episodes and recovers less well on less fertile sites. Ann. For. Sci. 71, 697–708. https://doi.org/10.1007/s13595-012-0220-5.

Tucker, C., 1979. Red and photographic infrared linear combinations for monitoring vegetation. Remote Sens. Environ. 8, 127–150.

UNDESA, United Nations, Department of Economic and Social Affairs. 2014. World Urbanization Prospects: The 2014 Revision, Highlights (ST/ESA/SER.A/352).

Vicente-Serrano, S.M., Beguería, S., López-Moreno, J.I., 2010. A Multi-scalar drought index sensitive to global warming: the Standardized Precipitation Evapotranspiration Index – SPEI. J. Clim. 23, 1696. https://doi.org/10.1175/2009JCLI2909.1.

Vogt, J., 2020. Urban forests as social-ecological systems. Encycl. World'S. Biomes 5 58–70. https://doi.org/10.1016/B978-0-12-409548-9.12405-4.

Voltas, J., Camarero, J.J., Carulla, D., Aguilera, M., Oriz, A., Ferrio, J.P., 2013. A retrospective, dual-isotope approach reveals individual predispositions to winter-drought induced tree dieback in the southernmost distribution limit of Scots pine. Plant Cell Environ. 36, 1435–1448.

Wang, J., Sammis, T.W., Gutschick, V.P., Gebremichael, M., Dennis, S.O., Harrison, R.E., 2010. Review of satellite remote sensing use in forest health studies. TOGEOGJ 3, 28–42.

White, J.C., Wulder, M.A., Hobart, G.W., Luther, J.E., Hermosilla, T., Griffiths, P., Coops, N.C., Hall, R.J., Hostert, P., Dyk, A., et al., 2014. Pixel-based image compositing for large-area dense time series applications and science. Can. J. Remote Sens. 40, 192–212.

Wigley, T.M.L., Briffa, K.R., Jones, P.D., 1984. On the average value of correlated time series, with applications in Dendroclimatology and Hydrometeorology. J. Appl. Meteorol. Clim. 23, 201–213.

Wu, Q., Zaw, Z., Yang, J., Yang, R., Li, Z., Hauer, R.J., Li, H., Fan, Z., Lu, H., Sterck, F., 2025. Urbanization associated with greater tree growth declines in urban than in rural forests. Urban For. Urban Green. 104, 128599.

Xoplaki, E., Gonzalez-Rouco, F., Luterbacher, J., Wanner, H., 2004. Wet season Mediterranean precipitation variability: influence of large scale dynamics and trends. Clim. Dyn. 23, 63–78. https://doi.org/10.1007/s00382-004-0422-0.

Yamaguchi, D.K., 1991. A simple method for cross-dating increment cores from living trees. Can. J. For. Res. 21, 414–416. https://doi.org/10.1139/x91-053.

Zhu, Z., Woodcock, C.E., 2012. Object-based cloud and cloud shadow detection in landsat imagery. Remote Sens. Environ. 118, 83–94.